

Dimer buckling induced by single-dimer vacancies on the Si(001) surface near T_c

Takashi Yokoyama

Takayanagi Particle Surface Project, ERATO, Japan Science and Technology Corporation, 3-1-2 Musashino, Akisima, Tokyo 196, Japan

Kunio Takayanagi

Takayanagi Particle Surface Project, ERATO, Japan Science and Technology Corporation,

3-1-2 Musashino, Akisima, Tokyo 196, Japan

and Material Science and Engineering, Tokyo Institute of Technology, 4259 Nagatsuta, Midori-ku, Yokohama 227, Japan

(Received 25 April 1997)

We used a low-temperature scanning tunneling microscope to observe a single-dimer vacancy (A-type defect) induce buckling of the dimers on a Si(001) surface near $T_c \approx 200$ K. This dimer buckling always occurs in rows adjacent to the A-type defects near T_c , which simultaneously forms an out-of-phase boundary in the domain of a $c(4 \times 2)$ structure. However, the out-of-phase boundaries around the A-type defects disappear on the surface at 78 K. We discuss the nucleation and growth behavior of the dimer buckling around the A-type defect and the influence of the defects on the structural phase transition of a Si(001) surface. [S0163-1829(97)06640-X]

I. INTRODUCTION

The atomic details of a Si(001) surface have been widely studied due to their technological and scientific aspects. Elaborate theoretical studies and experimental results have revealed the surface to be reconstructed to a 2×1 dimer structure above room temperature.¹⁻⁵ Below $T_c \approx 200$ K, the 2×1 structure is transformed to a $c(4 \times 2)$ structure,^{6,7} which has the antiphase arrangement $\alpha\beta\alpha\beta$ of the buckled-dimer rows, as shown in Fig. 1.^{4,5,8} The dimers of the 2×1 structure appear symmetric in scanning tunneling microscope (STM) images at room temperature;^{2,3} this is attributed to the time average of the flip-flop motion of the buckled dimers.^{3-5,9-11} Therefore, the phase transition from a 2×1 to a $c(4 \times 2)$ structure is considered to be the order-disorder transition of the buckled dimers.^{6,7,12-15}

Even at room temperature, STM observations have been revealed buckled dimers near atomic steps, kinks, and surface defects.^{3,16,17} Several reports have been suggested that surface defects play a significant role in the phase transition.^{7,14,15,18-22} Wolkow demonstrated that symmetric-appearing dimers still remained in many places on a high-defective surface (5–10%) well below T_c (120 K),²⁰ whereas Tochiwara *et al.* observed that decreasing the defect density to around 1% led to a large-size $c(4 \times 2)$ domain at 144 K.²³

Several studies have clarified the influence of individual defects on the dimer buckling at low temperatures.^{23,24} Among the three types of defects, single-dimer vacancy (A-type defect), double-dimer vacancy (B-type defect), and double-atom vacancy along the dimer row (C-type defect),¹⁶ the C-type defect induces local buckling of the dimers at room temperature.^{16,23} However, the C-type defect obstructs extensive formation of the $c(4 \times 2)$ arrangement below T_c .²³ This is explained by the fact that the C-type defect acts as a ‘‘phase shifter’’ by a half wavelength along the buckled-dimer row.^{23,25}

On the reconstructed Si(001) surface, the A-type defects are difficult to be removed even if special attention is paid to

preparing a clean surface, because the defects reduce the number of dangling bonds, resulting in the surface energy reduction at the cost of increased local strain.¹¹ Therefore, it is important to clarify the influence of the defects on the ordering of the buckled dimers. At room temperature, the A-type defect does not cause any detectable buckling of the dimers in adjacent regions.¹⁶ Tochiwara *et al.* suggested that the A-type defect would not have an effect on the buckling at low temperatures, based on their STM images of a complete $c(4 \times 2)$ ordering around the defect at 144 K.²³ In contrast, Uchikawa *et al.* observed several types of buckled dimers in the row of the A-type defect as well as symmetric-appearing dimers at 80 K.²⁴ These inconsistent results may be caused by the weak influence of A-type defects on the buckling, because A-type defects do not induce buckling at room temperature. We therefore observed the structural change of dimers around the A-type defects in a temperature range of 78–300 K.

In this study we report the results of STM observations on

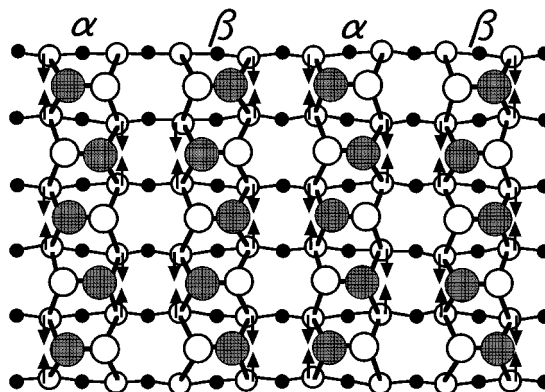


FIG. 1. Top view of the $c(4 \times 2)$ structure. Shaded circles indicate buckled atoms. The antiphase arrangement, denoted by $\alpha\beta\alpha\beta$, of the buckled-dimer rows is stabilized by displacement of the second-layer atoms, as denoted by arrows.

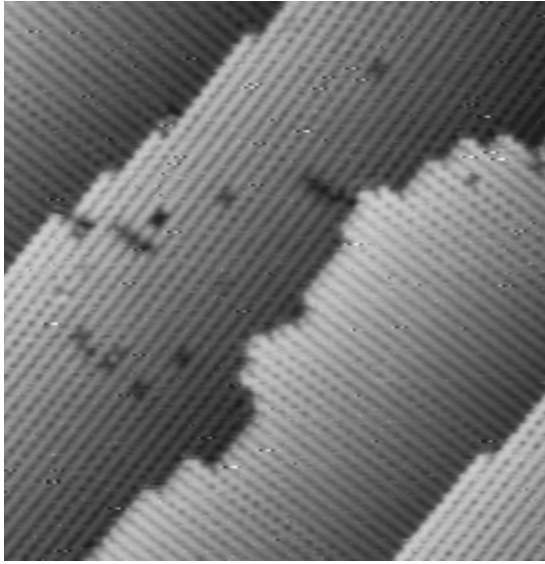


FIG. 2. Filled-state STM image on a Si(001) surface at 195 K. The image extends over $29 \times 29 \text{ nm}^2$.

a Si(001) surface at 195, 172, and 78 K, which indicate that A-type defects induce dimer buckling near T_c . We then discuss nucleation and growth of the dimer buckling induced by the A-type defects and the influence of the defects on the phase transition.

II. EXPERIMENT

Our experiments were performed in an ultrahigh-vacuum chamber with a base pressure of less than $4 \times 10^{-9} \text{ Pa}$ at room temperature. An antimony-doped Si(001) wafer of $0.05\text{--}0.09 \Omega \text{ cm}$ was employed as a sample for our observations. The sample was flashed up to 1450 K after being degassed at 850 K for 20 h and then cooled to room temperature at a rate of 3 K/s. This careful preparation, which was performed below $1 \times 10^{-8} \text{ Pa}$, created a low-defect surface density (below 1%). The clean sample was transferred into the low-temperature STM and was maintained at working temperatures for over 6 h to prevent thermal drifts and inaccurate temperature measurements. The filled-state STM images were then obtained by a constant current mode of 100 pA with a sample voltage of -1.5 V .

III. RESULTS AND DISCUSSION

At room temperature, we observed symmetric-appearing dimers on most of the surface, as well as buckled dimers only near the atomic-step edges, kinks, and C-type defects, which agreed with previous reports.^{2,3,16,17} On the surface at 195 K in Fig. 2, the buckled-dimer regions were expanded, compared to the STM images at room temperature, whereas symmetric-appearing dimers still remained. The defect density of the surface, estimated to be below 1%, was smaller than that of typical surfaces.^{3,16,21,23} Most defects in Fig. 2 appear as A-type defects.

Around the A-type defects of the surface near T_c (such as in Fig. 2), we found a different type of dimer buckling, which was not observed at room temperature. Figure 3(a) shows the following three characteristic features of the buck-

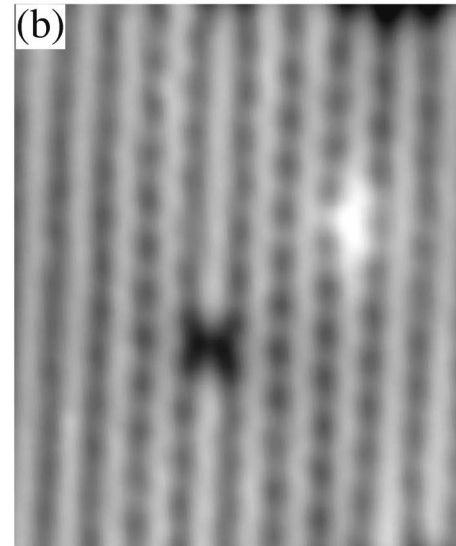
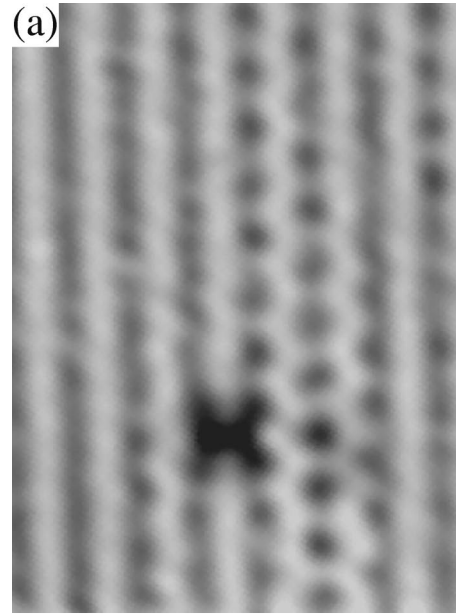


FIG. 3. Filled-state STM images of an A-type defect at (a) 195 K and (b) 172 K. The images in (a) and (b) extend over $4.8 \times 8.0 \text{ nm}^2$ and $6.7 \times 8.2 \text{ nm}^2$, respectively. Buckled dimers appear in rows adjacent to the defect, whereas dimers in the row of the defect appear symmetric.

ling around the defects: (i) the buckled dimers appear in rows adjacent to the defect, (ii) these buckled-dimer rows have mirror symmetry with respect to the dimer row of the defect, and (iii) the dimers in the row of the defect appear symmetric. Based on the STM image in Fig. 3(a), we constructed a structural model around the A-type defect in Fig. 4. The dimers in row S of the defect appear symmetric and those in the adjacent rows are buckled with α - and β -type configurations. Thus the dimer rows have an ordering of $\alpha S \beta$ ($\beta S \alpha$) around the A-type defect, as denoted in Fig. 4.

The origin of the dimer buckling around the A-type defects is well explained by their strain field. The A-type defect is a single-dimer vacancy, which results in dimerization of the second-layer atoms to reduce the number of their dan-

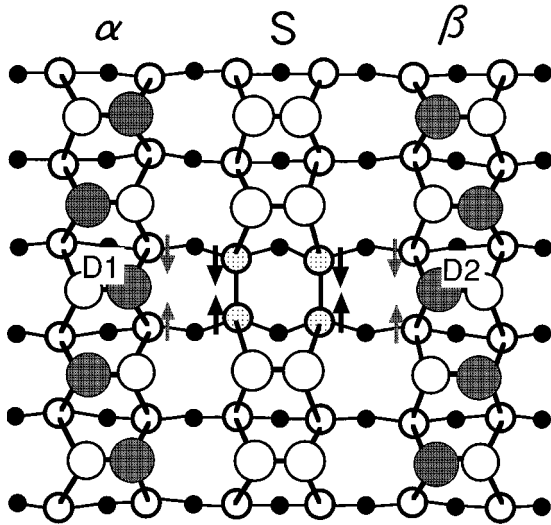


FIG. 4. Top view of the A-type defect. Solid arrows indicate the direction of the displacement of the second-layer atoms at the defect. This displacement induces a strain field such as that denoted by shaded arrows.

gling bonds.^{4,26,27} As denoted by arrows in Fig. 4, this dimerization induces a strain field around the defect such that the atom of the dimers $D1$ ($D2$) closer to the defect is raised. The strain field, however, is not so large that the buckling of dimers $D1$ and $D2$ is induced at room temperature. On the surface near T_c , dimers $D1$ and $D2$ are buckled and the buckling is expanded along the dimer row due to a strong “intra-row” (dimer-dimer) interaction. When the surface temperature is decreased below T_c , the $c(4 \times 2)$ domains grow to the left and right of the defect through an “inter-row” (row-row) interaction, as seen in Fig. 3(b).

Since the $c(4 \times 2)$ domains grow from individual A-type defects, they interact with each other near T_c . In-phase and out-of-phase interactions between two A-type defects in the same row are seen in Figs. 5(a) and 5(b), respectively. The in-phase interaction enhances the buckling, as schematically shown in Fig. 5(c). On the other hand, the out-of-phase interaction weakens the buckling, thereby dimers near the defects appear symmetric, as seen in Figs. 5(b) and 5(d). In the case of the enhanced (weakened) buckling, an odd (even) number of dimers exists in a row between two defects.²⁸

The in-phase and out-of-phase interactions also occur when the A-type defects are not in the same row, as shown in Fig. 6. The $c(4 \times 2)$ domains from the upper defect A1 in the image interact with those from the lower defect A2 at 172 K. The right-side domain of the lower defect A2 is affected by the in-phase and out-of-phase interaction with the left and right domains of the upper defect A1. Consequently, the dimers on the right-hand side of the upper defect A1 appear symmetric in Fig. 6, due to the out-of-phase interaction.

Another interesting feature is that A-type defects produce an ordering of $\alpha\beta\alpha S\beta\alpha\beta$ near T_c , which is separated by the symmetric-appearing dimer row, as shown in Fig. 3(b). However, on the surface at 78 K [see Fig. 7(b)], we observed neither the symmetric-appearing dimers in row S nor the out-of-phase boundary $\alpha\alpha$ ($\beta\beta$) at the defect. This indicates that the ordering of $\alpha S\beta$ near the defect has changed into

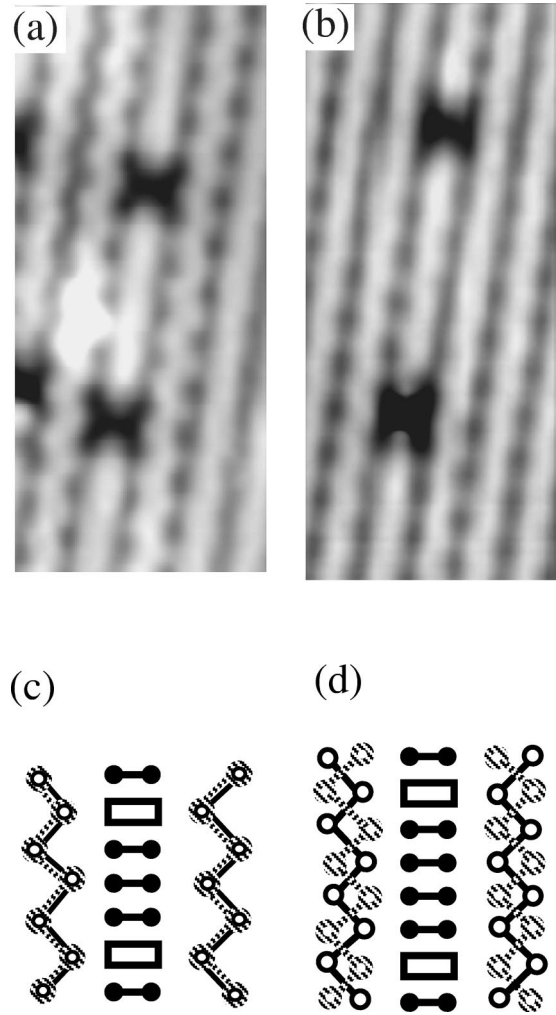


FIG. 5. (a) In-phase and (b) out-of-phase interactions between two A-type defects in the same row. The images extend over $3.5 \times 7.6 \text{ nm}^2$. Nine and twelve dimers exist between the defects in (a) and (b), respectively. The weakened buckling of dimers adjacent to the defects was observed in (b) due to the out-of-phase interaction. (c) and (d) are schematic illustrations of the in-phase and out-of-phase interactions, respectively. Open circles indicate buckled atoms from the lower defect and hatched circles indicate those from the upper defect in (c) and (d).

that of $\alpha\beta\alpha$ or $\beta\alpha\beta$ at 78 K. The inter-row interaction of the buckled-dimer rows is sufficiently strong to overcome the strain-field effect of the A-type defect at 78 K. On the surface at 172 K of Fig. 7(a), we observed the ordering of $\alpha\beta\beta$ at the A-type defect resulting from the competition between the inter-row interaction and the strain-field effect of the A-type defect. Uchikawa *et al.* may have observed this competition at 80 K, due to a large number of surface defects.²⁴ In contrast, Tochihara *et al.* obtained a complete $c(4 \times 2)$ ordering at 144 K, as shown in Fig. 7(b).²³

Finally, we consider the influence of the A-type defects on the phase transition of the surface. An A-type defect generates nucleation of the dimer buckling in the two rows adjacent to the defect near T_c , which simultaneously forms an out-of-phase boundary. The phase boundary is also formed by an out-of-phase interaction between the defects, as shown in Figs. 5(b) and 6. This study suggests that an increase in A-type defects generates many out-of-phase boundaries. The

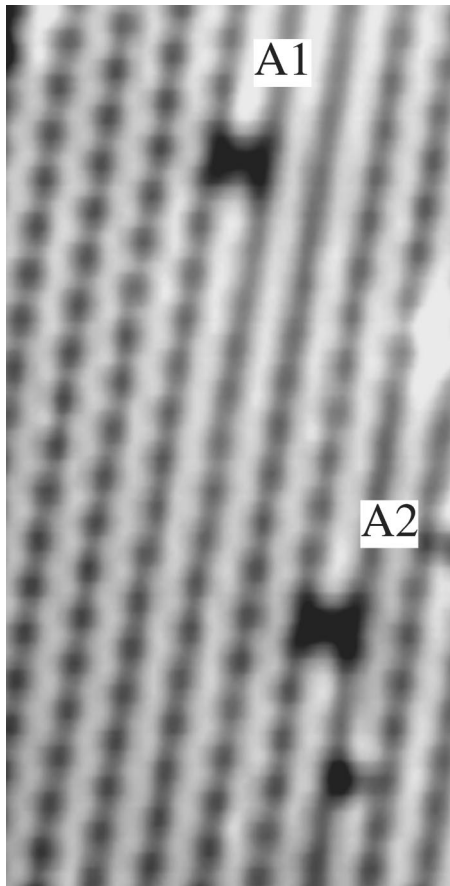


FIG. 6. In-phase and out-of-phase interaction between the $c(4 \times 2)$ domains from A-type defects A1 and A2 at 172 K. The image extends over $5.6 \times 10.9 \text{ nm}^2$.

presence of many phase boundaries appears to smear out the transition. Accordingly, symmetric-appearing dimers remained in a wide region on a surface containing numerous defects even at 120 K.²⁰ More details regarding the influence of A-type defects on the phase transition will be clarified by Monte Carlo simulations based on an Ising-spin model.²⁹

IV. CONCLUSION

Using a low-temperature STM, we observed the effects of the A-type defect that contribute to dimer buckling on a Si(001) surface near T_c . We discovered that A-type defects induced dimer buckling in rows adjacent to the defects on the surface near T_c , which was not observed at room temperature. We explained that the strain field at the A-type

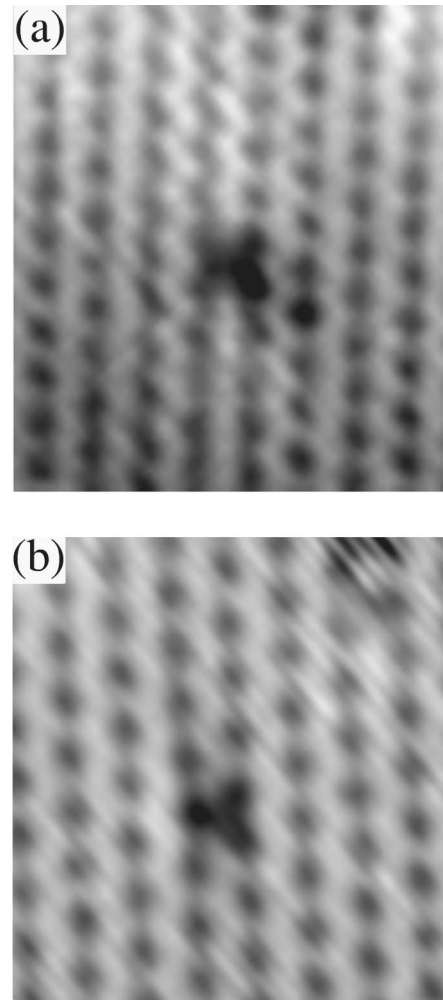


FIG. 7. Filled-state STM images around an A-type defect at (a) 172 K and (b) 78 K. The images extend over $5.9 \times 6.6 \text{ nm}^2$.

defect induced dimer buckling in rows adjacent to the defect. For an isolated A-type defect, the strain-field effect was not strong for the A-type defect to induce buckling at room temperature and 78 K. Thus the A-type defect only affects buckling of dimers near T_c .

ACKNOWLEDGMENTS

We would like to thank M. Okamoto and H. Ohnishi for useful discussion. We also thank W.-S. Cho for his critical reading of this manuscript.

¹R. E. Schiler and H. E. Farnsworth, *J. Chem. Phys.* **30**, 917 (1959).

²R. M. Tromp, R. J. Hamers, and J. E. Demuth, *Phys. Rev. Lett.* **55**, 1303 (1985).

³R. J. Hamers, R. M. Tromp, and J. E. Demuth, *Phys. Rev. B* **34**, 5343 (1986).

⁴D. J. Chadi, *Phys. Rev. Lett.* **43**, 43 (1979).

⁵K. C. Pandey, in *Proceedings of the 17th International Confer-*

ence on Physics of Semiconductors, edited by D. J. Chadi and W. A. Harrison (Springer, New York, 1985), p. 55.

⁶T. Tabata, T. Aruga, and Y. Murata, *Surf. Sci.* **179**, L63 (1987).

⁷M. Kubota and Y. Murata, *Phys. Rev. B* **49**, 4810 (1994).

⁸M. Needels, M. C. Payne, and J. D. Joannopoulos, *Phys. Rev. Lett.* **58**, 1765 (1987).

⁹H.-J. Guntherodt and R. Wiesendanger, *Scanning Tunneling Microscope I*, 2nd ed. (Springer-Verlag, Berlin, 1994), p. 93.

- ¹⁰J. A. Kubby and J. J. Borland, *Surf. Sci. Rep.* **26**, 61 (1996).
- ¹¹H. Neddermeyer, *Rep. Prog. Phys.* **59**, 701 (1996).
- ¹²J. Ihm, D. H. Lee, J. D. Joannopoulos, and J. J. Xiong, *Phys. Rev. Lett.* **51**, 1872 (1983).
- ¹³A. Saxena, E. T. Gawlinski, and J. D. Gunton, *Surf. Sci.* **160**, 618 (1985).
- ¹⁴K. Inoue, Y. Morikawa, K. Terakura, and M. Nakayama, *Phys. Rev. B* **49**, 14 774 (1994).
- ¹⁵K. Terakura, T. Yamasaki, and Y. Morikawa, *Phase Transit.* **53**, 143 (1995).
- ¹⁶R. J. Hamers and U. Köhler, *J. Vac. Sci. Technol. A* **7**, 2854 (1989).
- ¹⁷H. Tochiohara, T. Sato, T. Sueyoshi, T. Amakusa, and M. Iwatsuki, *Phys. Rev. B* **53**, 7863 (1996).
- ¹⁸F. H. Stillinger, *Phys. Rev. B* **46**, 9590 (1992).
- ¹⁹J. Alvarez, V. H. Etgens, X. Torrelles, H. A. van der Vegt, P. Fajardo, and S. Ferrer, *Phys. Rev. B* **54**, 5581 (1996).
- ²⁰R. A. Wolkow, *Phys. Rev. Lett.* **68**, 2636 (1992).
- ²¹D. Badt, H. Wengelink, and H. Neddermeyer, *J. Vac. Sci. Technol. B* **12**, 2015 (1994).
- ²²Y. Imry and S.-K. Ma, *Phys. Rev. Lett.* **24**, 1399 (1975).
- ²³H. Tochiohara, T. Amakusa, and M. Iwatsuki, *Phys. Rev. B* **50**, 12 262 (1994).
- ²⁴M. Uchikawa, M. Ishida, K. Miyabe, K. Hata, R. Yoshizaki, and H. Shigekawa, *Surf. Sci.* **357-358**, 468 (1996).
- ²⁵Y. Nakamura, H. Kawai, and M. Nakayama, *Phys. Rev. B* **52**, 8231 (1995).
- ²⁶N. Robert and R. J. Needs, *Surf. Sci.* **236**, 112 (1990).
- ²⁷J. Wang, T. A. Arias, and J. D. Joannopoulos, *Phys. Rev. B* **47**, 10 497 (1993).
- ²⁸In Fig. 3 the weak buckling of dimers on the left-hand side of the defect is explained by the out-of-phase interaction with another A-type defect on the upper side of the image (not shown).
- ²⁹M. Okamoto, T. Yokoyama, and K. Takayanagi (unpublished).